Supporting Information

Metal-Support Interactions in Pt-Embedded Porous Fe_2P Nanorods for Efficient Hydrogen Production

Ahmed Mahmoud Idris [a,1], *Song Zheng* [a,1], *Meng Zhang* [b], *Xinyan Jiang* [b], *Guocan Jiang* [b,c], *Jin Wang* [b], *Sheng Li* [a,c], *Zhengquan Li* [a,b,c,*]

[a] *Department of Physics, Zhejiang Normal University, Jinhua, Zhejiang 321004, PR China*

[b] *Key Laboratory of the Ministry of Education for Advanced Catalysis Materials, Zhejiang Normal University, Jinhua, Zhejiang 321004, P. R. China.*

[c] *Zhejiang Institute of Photoelectronics, Zhejiang Normal University, Jinhua, Zhejiang 321004, PR China.*

*Corresponding author E-mail: zqli@zjnu.edu.cn

1- Chemicals and reagents

All the chemicals and reagents used in this work are analytical grade (used as received without further purification). The aqueous solutions were prepared with 18.2 MΩ deionized water. Terephthalic acid (99.8%), N, N-dimethylacetamide (DMA, 99.8%), cyclohexane (99.5%), and Eosin-Y (EY, 97%) were purchased from Aladdin Company. Iron (III) chloride hexahydrate ($FeCl_3 \cdot 6H_2O$, 99%), Absolute ethanol (99.5%), Triethanolamine (TEOA, 98%), Hexachloroplatinic acid (H_2PtCl_6, 99.5%), sodium hypophosphite ($NaH_2PO_2 \cdot H_2O$, 99.5%) were purchased from Sinopharm Chemical.

2- Characterizations

Scanning electron microscopy (SEM) was performed on a Hitachi S-4800 scanning electron microscopy. Transmission electron microscopy (TEM) was conducted on a JEOL 2010F transmission electron microscopy. X-ray powder diffraction (XRD) patterns were recorded on a Philips X'Pert X-ray diffractometer with Cu Kα radiation. UV-vis absorption spectra were measured on an ultraviolet spectrophotometer (Hitachi UV-2600). Steady-state photoluminescence spectra were recorded on a Hitachi H-4600 spectrometer with a Xe lamp.

3- Photocatalytic Hydrogen Production Measurement

The photocatalytic H_2 production was carried out in a 30 mL Pyrex reaction cell with a branch pipe for vacuuming and inputting gas at room temperature (20 ºC). The irradiation source is a 300 W Xe lamp (PLS-SXE300, Beijing Perfect light, set at 100 mW cm^{-2}) equipped with a UV cutoff filter to obtain visible light (≥ 420 nm). In a typical procedure, 5 mg of catalysts and 20 mg of eosin-Y (EY) were loaded in the cell, evacuated for 5 minutes, and flooded with Ar for 10 minutes. Next, 9 mL of DI water and 1 mL of triethanolamine (TEOA) were injected into the cell, and the pH value of the solution was about 9.6. The solution was then evacuated, flooded with Ar gas twice, and irradiated under the Xe lamp to initiate the photocatalytic process. After being irradiated for a certain period, the gas produced in the cell was analyzed by gas chromatography (Agilent 7820B, Ar as the carrier gas) with a thermal conductivity detector. The concentration of the gas product was determined using a standard curve

that the common gases had calibrated.

The apparent quantum yield (AQY) was measured under the same photocatalytic reaction conditions and illumination is provided by 300 W xenon lamp with a monochromator.

$$AQY\ [\%] = \frac{Number\ of\ evolved\ H2\ \times\ 2}{Number\ incident\ photons} x100$$

4- Photoelectrochemical measurements

Photocurrent measurement and electrochemical impedance spectroscopy (EIS) were performed on a CHI 660D electrochemical workstation (Shanghai Chenhua, China) with a three-electrode system using the sample-coated fluorine-doped tin oxide (FTO) glass as a photoelectrode, Pt foil as a counter electrode, and the Ag/AgCl electrode as a reference electrode, respectively. For the linear sweep voltammetry (LSV) test, the graphite rod was used as the counter electrode instead of Pt foil on the electrochemistry workstation. The working electrode was prepared by dip-coating method, and 0.5 mol/L of Na_2SO_4 solution (pH = 6.8) was used as the electrolyte. Typically, 1 mg of the catalyst was dispersed into 0.5 mL of ethanol and 10 μL of Nafion solution to form a slurry. Then, the slurry was dip-coated on the clean FTO conductive glass with an exposure area of 1 cm^2. Subsequently, the film was dried in a vacuum oven at 60 ºC.

5- DFT calculations

The density functional theory (DFT) simulations were computed using the Vienna Ab initio Simulation Package (VASP).[1] The electron-ion interactions are described by the projector-augmented wave (PAW) pseudopotentials method.[2] The generalized gradient approximation (GGA) for the exchange-correlation energy was computed by the Perdew Burke Ernzerhof functional (PBE).[3] The energy cutoff of 600 eV was adopted to optimize the bulk with Monkhorst-Pack grid of Fe_2P are 5×5×7. Pt is 11×11×11 until the maximal residual force and energy of each atom should be less than 0.05 eV/Å and 1.0 $\times 10^{-6}$ eV/atom. The optimized lattice parameters of a = b =5.80337, c = 3.42706 Å for Fe_2P bulk are close to the experimental value of conventional cell a

= b = 5.8685Å, c = 3.4571. The obtained lattice parameters of a = b = c =3.96751 Å for Pt is similar to the experimental value of conventional cell a = b = c =3.9231 Å. To simulate the adsorbed H atom (termed as H*) one clean Fe_2P (001) surface, Pt (111) surfaces, and Pt-Fe_2P surface. The slab model of Fe_2P (001) consists of 60 Fe and 32 P atoms, the vacuum is set to at least 20 Å, and the calculations are modeled with the k-point of 2× 2×1. The top two layers were allowed to relax, while the bottom three layers were fixed during the calculations. The slab model of Pt (111) consists of 80 Pt atoms, the vacuum is set to at least 20 Å, and the calculations are modeled with the k-point of 3×3×1. The slab model of Pt-Fe_2P consists of 60 Fe, 32 P, and 4 Pt atoms, and the calculations are modeled with the k-point of 2× 2×1. The top two layers were allowed to relax, while the bottom three layers were fixed during the calculations. The energy cutoff of 400 eV was adopted to optimize the slab until the maximal residual force and energy of each atom should be less than 0.05 eV/Å and 1.0 $\times 10^{-5}$ eV/atom. The free energies of the systems were computed by

$$\Delta G_{H^*} = \Delta E_{H^*} + \Delta ZPE - T\Delta S$$

where ΔE_{H^*}, ΔZPE, and $T\Delta S$ are the adsorption energy, the difference in zero-point energy between the adsorbed and the gas phase, and vibrational entropy energy due to the H* adsorption, respectively. The Gibbs free energy was corrected at a temperature of 298 K.

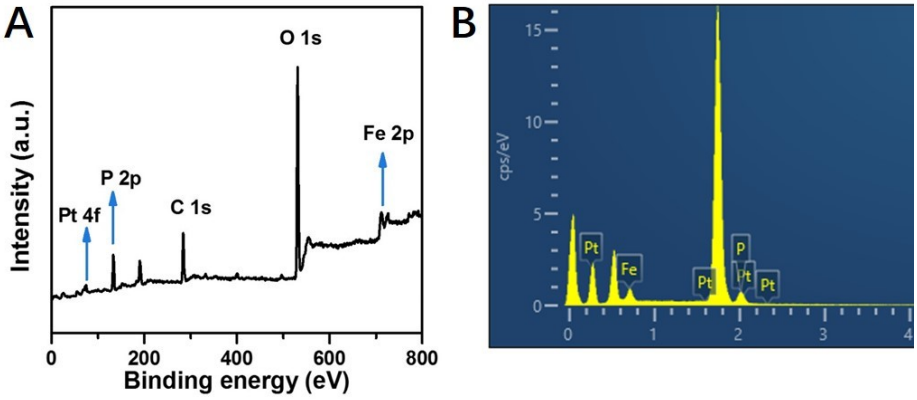

Figure S1. (A) Full-range XPS survey spectra of MSI Pt-Fe_2P.(B) EDX of MSI Pt-Fe_2P.

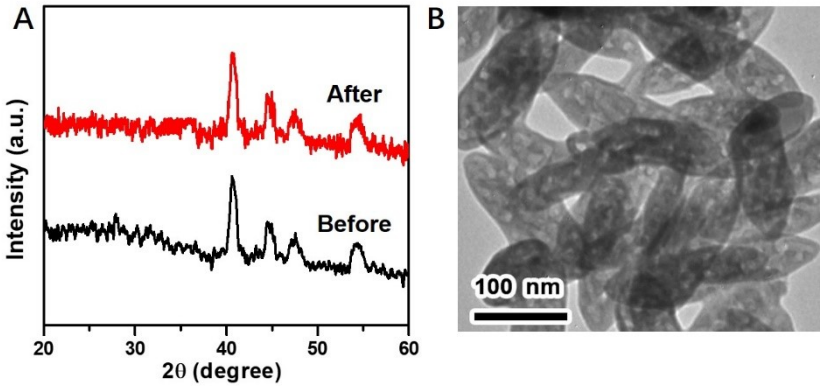

Figure S2. (A) XRD spectra of MSI Pt-Fe_2P, (B) TEM of MSI Pt-Fe_2P after the photocatalytic recycling reaction.

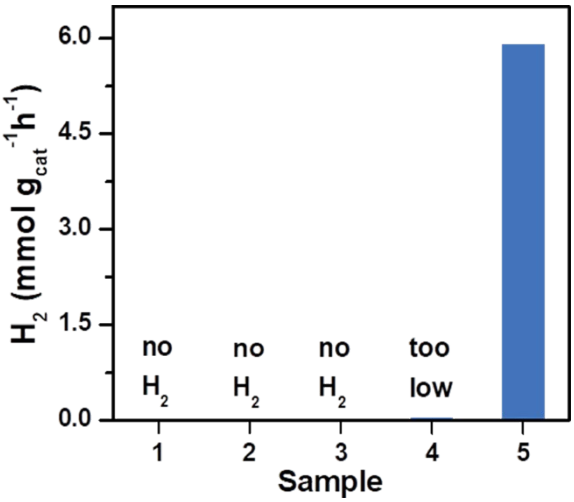

Figure S3. Control photocatalytic experiments by changing one of the following conditions: (1) without light irradiation; (2) without sacrificial agents; (3) without dyes; (4) without catalysts; (5) without changing any photocatalytic conditions.

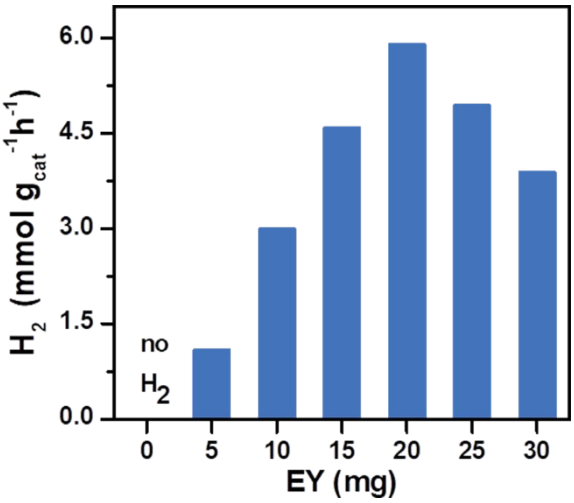

Figure S4. Photocatalytic H_2 production of MSI Pt-Fe_2P with different EY amounts.

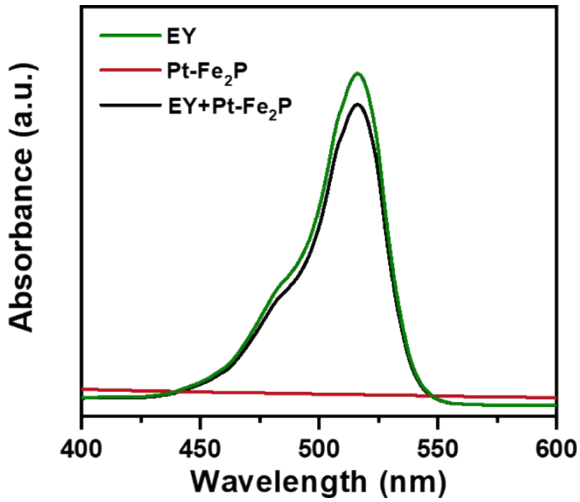

Figure S5. UV–vis spectra of EY, MSI Pt-Fe_2P and EY+ MSI Pt-Fe_2P.

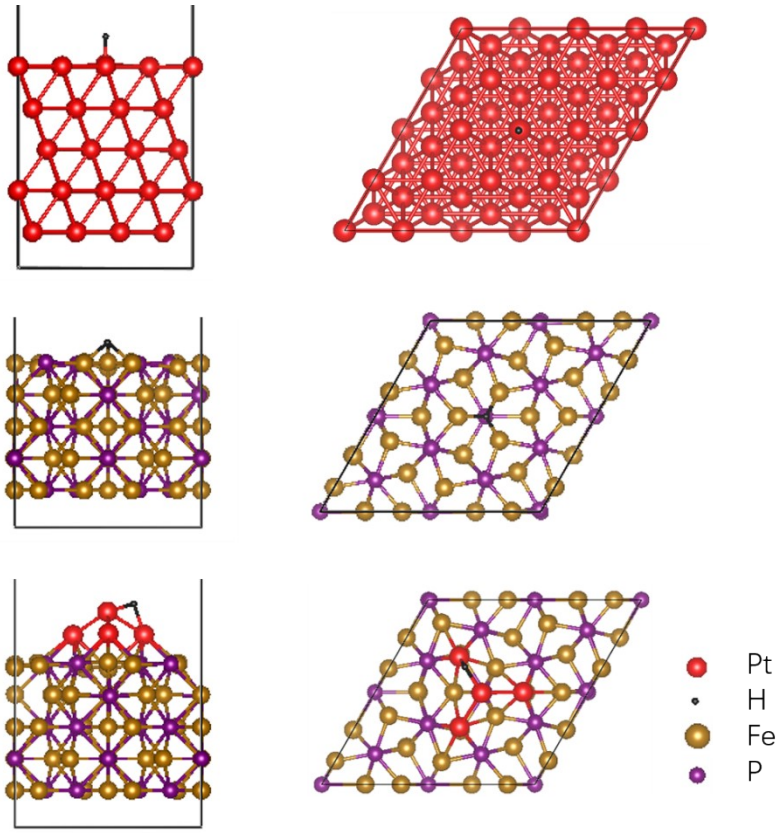

Figure S6. Structures for the Pt, Fe_2P, and MSI Pt-Fe_2P intermediates, respectively.

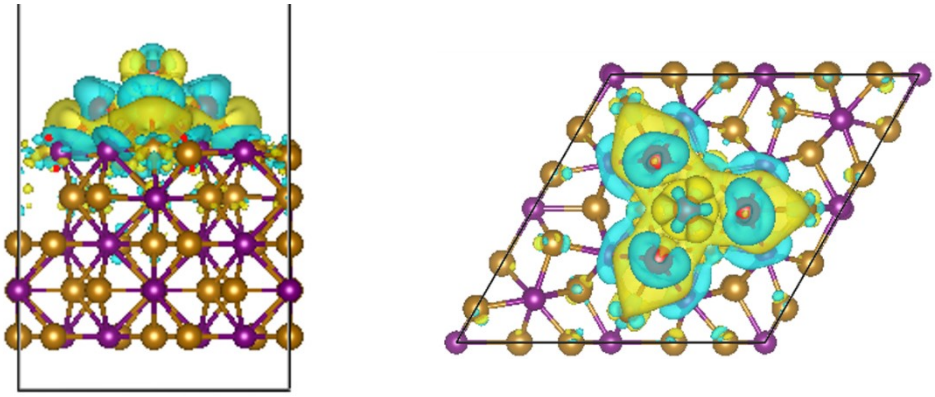

Figure S7. Charge density difference of MSI Pt-Fe_2P.

Table S1. Element concentration of Fe_2P and MSI Pt-Fe_2P measured by XRF.

Element	Fe_2P	MSI Pt-Fe_2P
Fe	56.2634 %	66.5920%
P	43.7366%	31.9360 %
Pt	0%	1.4720 %

Table S2. Comparison of the reported photocatalytic H_2 production of typical dye-sensitized catalysts and semiconductor photocatalysts.

Catalysts	Dye	Rat of H_2 μmol $h^{-1}g^{-1}$	Ref
$Pt/K_{0.80}Ti_{1.71}Li_{0.29}O_{3.97}$	$Ru(bpy)_3^{2+}$	2.4	4
RGO/Pt	$Ru(dcbpy)_3^{2+}$	2.53	5
TiO_2/RGO/Pt	$Ru(dcbpy)_3^{2+}$	191.8	6
Ti–MCM-48	$Ru(bpy)_2(dcbpy)(PF_6)_2$	13.3	7
Pt/MWCNT	Eosin Y	3.4	8
Co/TiO_2	Rhodamine B	227.3	9
Pt/UiO-66(Zr) (MOF)	Rhodamine B	116	10
RGO	Eosin Y	0.4	11
MIL-53	Eosin Y	315	12
Pt/NH_2-MIL-101 (Gr)	Rhodamine B	4.77	13
$rGO/MOF/Ni_4S_3$	Eosin Y	56	14
MoS_2 /NH_2-UiO-66/G	Eosin Y	62.12	15
Ni-doped Fe_3S_4	Eosin Y	3375	16
Fe-Ni-P		5400	-
$Pt/SrTiO_3$		491.5	17
MoO_3/MIL-125-NH_2	No	400	18
Cd-PBA	No	13600	19
MSI Pt-Fe_2P	**Eosin Y**	**6000**	**This work**

References

1. G. Kresse and D. J. P. r. b. Joubert, *Phys. Rev*, 1999, **59**, 1758-1775.
2. P. E. J. P. r. B. Blöchl, *Phys. Rev*, 1994, **50**, 17953 -17979.
3. J. P. Perdew, K. Burke and M. J. P. r. l. Ernzerhof, *Phys. Rev. Lett*, 1996, **77**, 3865-3868.
4. M. Matsuoka, Y. Ide and M. Ogawa, *Phys. Chem. Chem. Phys*, 2014, **16**, 3520-3522.
5. M. Zhu, Y. Dong, B. Xiao, Y. Du, P. Yang and X. Wang, *J. Mater. Chem*, 2012, **22**, 23773-23779.
6. Y. Chen, Z. Mou, S. Yin, H. Huang, P. Yang, X. Wang and Y. Du, *Mater. Lett*, 2013, **107**, 31-34.
7. S. Rasalingam, R. Peng, C.-M. Wu, K. Mariappan and R. T. Koodali, *Catal. Commun*, 2015, **65**, 14-19.
8. Q. Li, L. Chen and G. Lu, *J. Phys. Chem. C*, 2007, **111**, 11494-11499.
9. T. T. Le, M. S. Akhtar, D. M. Park, J. C. Lee and O. B. Yang, *Appl. Catal., B*, 2012, **111-112**, 397-401.
10. J. He, J. Wang, Y. Chen, J. Zhang, D. Duan, Y. Wang and Z. Yan, *Chem. Commun*, 2014, **50**, 7063-7066.
11. Z. Mou, Y. Dong, S. Li, Y. Du, X. Wang, P. Yang and S. Wang, *Int. J. Hydrog. Energy*, 2011, **36**, 8885-8893.
12. S. Li, F. Wu, R. Lin, J. Wang, C. Li, Z. Li, J. Jiang and Y. Xiong, *Chem. Eng. J*, 2022, **429**, 132217.
13. M. Wen, K. Mori, T. Kamegawa and H. Yamashita, *Chem Commun*, 2014, **50**, 11645-11648.
14. D. Liu, Z. Jin, Y. Zhang, G. Wang and B. Ma, *J. Colloid. Interf. Sci*, 2018, **529**, 44-52.
15. X. Hao, Z. Jin, H. Yang, G. Lu and Y. Bi, *Appl. Catal., B*, 2017, **210**, 45-56.
16. M. Zhang, X. Chen, X. Jiang, J. Wang, L. Xu, J. Qiu, W. Lu, D. Chen and Z. Li, *ACS Appl. Mater. Interfaces*, 2021, **13**, 14198-14206.
17. K. Han, W. Li, C. Ren, H. Li, X. Liu, X. Li, X. Ma, H. Liu and A. Khan, *J. Taiwan Inst. Chem. E*, 2020, **112**, 4-14.
18. C. Zhang, C. Xie, Y. Gao, X. Tao, C. Ding, F. Fan and H. L. Jiang, *Angew. Chem. Int. Ed*, 2022, **61**, e202204108.
19. P. Zhang, D. Luan and X. W. Lou, *Angew. Chem. Int. Ed*,2020, **32**, 2004561.